T. Beyazoglu, T. O. Rocheleau, K. E. Grutter, A. J. Grine, M. C. Wu, and C. T.-C. Nguyen, "A multi-material *Q*-boosted low phase noise optomechanical oscillator," *Tech. Digest*, 2014 IEEE Int. Micro Electro Mechanical Systems Conference, San Francisco, California, Jan. 26-30, 2014, pp. 1193-1196.

A MULTI-MATERIAL *Q*-BOOSTED LOW PHASE NOISE OPTOMECHANICAL OSCILLATOR

Turker Beyazoglu, Tristan O. Rocheleau, Karen E. Grutter, Alejandro J. Grine, Ming C. Wu and Clark T.-C. Nguyen
University of California, Berkeley, USA

ABSTRACT

A Radiation Pressure driven Optomechanical Oscillator (RP-OMO) comprised of attached concentric rings of polysilicon and silicon nitride has achieved a first demonstration of a mixed material optomechanical device, posting a mechanical Q_m of 22,300 at 52 MHz, which is more than 2× larger than previous single-material silicon nitride devices [1]. With this Q_m, the RP-OMO exhibits a best-to-date phase noise of -125 dBc/Hz at 5 kHz offset from its 52-MHz carrier—a 12 dB improvement from the previous best by an RP-OMO constructed of silicon nitride alone [1]. The key to achieving this performance is the unique mechanical *Q*-boosting design where most of the vibrational energy is stored by the high-Q_m polysilicon inner ring which in turn boosts the overall Q_m over that of silicon nitride, all while retaining the high optical Q_o >190,000 of silicon nitride material. Simultaneous high Q_o and Q_m reduces the optical threshold power for oscillation, allowing this multi-material RP-OMO to achieve its low phase noise with an input laser power of only 3.6 mW.

INTRODUCTION

Recent advancements in cavity opto-mechanics have allowed researchers to exploit coupling between the optical field and mechanical motion of an optical cavity to affect cooling [2] or amplification [3] of mechanical motion. Cooling the mechanical motion of micro-scale objects has been of high scientific interest, since it facilitates observation and exploration of certain quantum phenomena, e.g., the standard quantum limit of detection [4]. On the other hand, amplification of the mechanical motion allows realization of micro-scale devices for practical applications, such as light-driven low-phase noise signal generation by radiation pressure driven optomechanical oscillators (RP-OMO's) [3] [5].

Indeed, the ability to achieve self-sustained oscillation with no need for feedback electronics makes an RP-OMO compelling for on-chip applications where directed light energy, e.g., from a laser, is available to fuel the oscillation. In addition to stand-alone oscillator applications, RP-OMO's have been suggested for deployment as combined mixer+oscillators in homodyne receivers and RF sub-carrier links [5], and as reference/microwave oscillators to reduce power consumption in chip scale atomic clocks (CSAC) [1].

To be useful in such applications, the output of an RP-OMO must be sufficiently stable, as gauged over short time spans by its phase noise. To date, the work of [1] achieves the best in class phase noise for such devices of -113 dBc at a 5-kHz offset from a 74-MHz carrier by maximizing the mechanical Q_m of its optomechanical structure—a result of recognizing that mechanical Q_m has the strongest impact on phase noise, much more than optical Q_o. However, the performance of [1], although good, is still not sufficient, mainly because it uses a single material (silicon nitride) to set both its mechanical and optical *Q*'s.

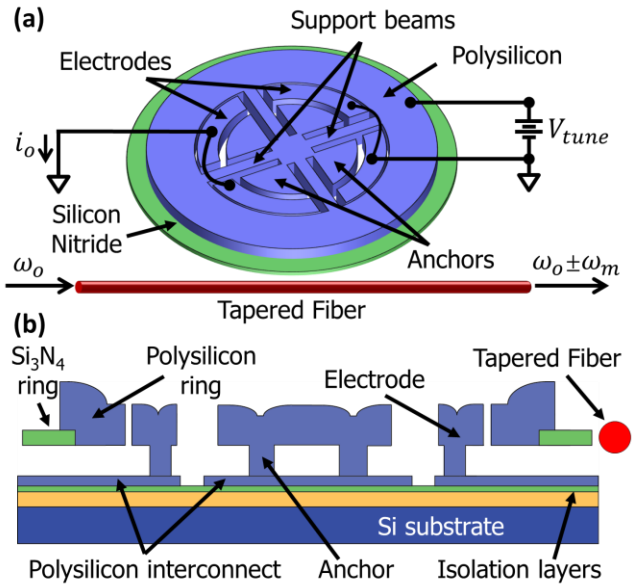

Fig. 1: (a) Perspective-view and (b) cross-sectional schematics of the Q-boosted RP-OMO. Here, the polysilicon inner ring is mechanically coupled at its outer edge to a concentric high optical Q_o silicon nitride ring. A tapered fiber provides optical coupling, while polysilicon electrodes inside the ring enable frequency tuning and electrical input-output.

The RP-OMO described in this work (*cf.* Fig. 1) circumvents this limitation by combining a nitride optical material with a lower mechanical loss polysilicon material that shares its energy to effectively boost the overall mechanical Q_m from 10,400 for a nitride device alone to 22,300. As a result of its high mechanical Q_m, the RP-OMO posts a phase noise of -125 dBc/Hz at 5 kHz offset from its 52-MHz carrier, which is 12 dB better than the previous state-of-the-art RP-OMO constructed of silicon nitride alone [1]. The doped polysilicon structure and electrodes additionally allow tuning of the RP-OMO's oscillation frequency via DC voltage as indicated by V_{tune} in Fig. 1(a), enabling future deployment of the multi-material RP-OMO as a locked oscillator in the targeted CSAC application [1] depicted in Fig. 2.

DEVICE STRUCTURE AND OPERATION

The *Q*-boosted RP-OMO, summarized in perspective-

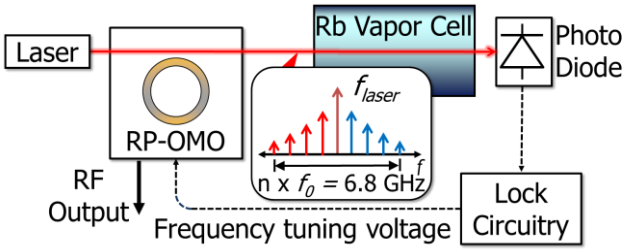

Fig. 2: Targeted CSAC application where an RP-OMO's higher harmonic locks to a Rb vapor cell to borrow its long term stability. Voltage controlled tunability of the RP-OMO provides a simple feedback mechanism for locking where the tuning voltage emanates from locking circuitry.

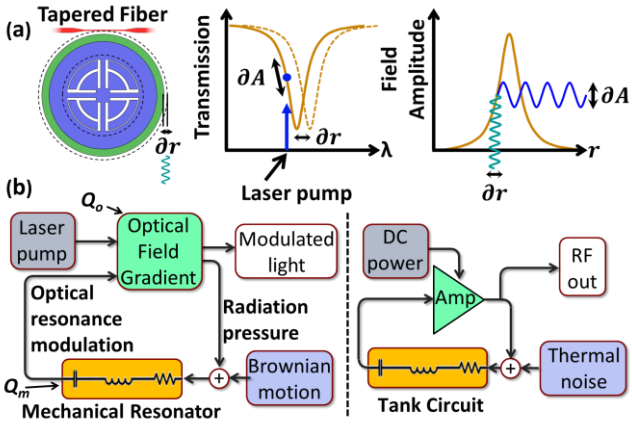

Fig. 3: (a) Optomechanical oscillator dynamics: Radiation pressure from light in the cavity changes the radius which in turn changes the optical field, raising the radiation pressure, and so on, to generate a growing cycle. (b) System block diagrams comparing an RP-OMO with an electronic oscillator. The dynamics of the RP-OMO is analogous to an electronic oscillator where the optical field (with the high Q_o resonance) sets the gain and the mechanical resonator serves as the tank circuit feedback element.

view and cross-section in Fig. 1, comprises a high mechanical Q_m polysilicon inner ring physically attached at its outer edge to a concentric high optical Q_o (but comparatively low mechanical Q_m) silicon nitride ring. Spokes attached to the inner edges of the polysilicon ring extend radially inwards to a common central anchor and serve to support the entire multi-ring device in a completely balanced fashion, where inward forces along the spokes are met with equal and opposite ones, cancelling energy leakage from the spokes to the substrate. Polysilicon electrodes inside the ring overlap its inner edge to form capacitive gaps that then allow electrical interrogation and control (in addition to optical).

To operate the device, an input laser is blue-detuned, i.e., at a wavelength slightly shorter, from the optical resonance of the nitride ring and coupled into the ring via a tapered fiber [6]. Enhanced by the Q_o, the circulating light generates a radiation pressure force that displaces the mechanical resonator which in turn shifts the optical resonance. As depicted in Fig. 3(a), initially Brownian mechanical motion modulates the optical pump field, which in turn generates a resonant radiation pressure force that modifies the mechanical dynamics. The coupling of the two degrees of freedom is described by the differential equations [5]:

$$\ddot{r}(t) + \Gamma_m \dot{r}(t) + \omega_m^2 r(t) = \frac{F_{rp}(t)}{m_{eff}} = \frac{1}{m_{eff}} \frac{2\pi n}{c} |A(t)|^2 \quad (1)$$

$$\dot{A}(t) + A(t)\left[\frac{\omega_o}{2Q_L} - i\Delta\omega + i\frac{\omega_o}{r_o} r(t)\right] = i\sqrt{\frac{\omega_o}{Q_e}}|S|^2 \quad (2)$$

where $r(t)$ is the radial displacement of the mechanical resonator from equilibrium, Γ_m is the mechanical damping rate, ω_m is the mechanical resonance frequency, n is the effective refractive index for the optical mode, c is the speed of light, $A(t)$ the optical field circulating in the optical cavity, $\Delta\omega$ the detuning of laser from optical resonance frequency ω_o, $|S|^2$ the input optical power, Q_L the loaded quality factor of the optical resonance, Q_e the quality factor associated with coupling loss, and m_{eff} the mode dependent effective mass of the mechanical resonator.

Effectively, the resonant radiation pressure force modifies the mechanical dynamics by acting as a negative mechanical damping that completely cancels out the intrinsic mechanical loss when the circulating optical power reaches a threshold value. From a feedback loop perspective, the optical pump power and Q_o sets the gain from the mechanical motion to the radiation pressure which gets positively fed back to the mechanical resonator as depicted in Fig. 3(b), which further shows how the RP-OMO is in fact not so different from a conventional MEMS oscillator. Indeed, in both cases, the MEMS resonator in positive feedback serves as an ultra-high-Q bandpass biquad that accentuates the signal at resonance while suppressing noise off resonance. In this regard, high Q_m is of utmost importance if either system is to exhibit low close-to-carrier phase noise as predicted by the well-known Leeson's equation [7]:

$$L(f) \cong 10\log\left[\frac{2FkT}{P_{sig}}\left(1 + \frac{1}{Q^2}\left(\frac{f_c}{2\Delta f}\right)^2\right)\right] \quad (3)$$

where $L(f)$ is the single side-band phase noise at an offset Δf from the carrier frequency f_c. F is a fitting parameter often termed as effective noise figure, k is the Boltzmann's constant, T is the absolute temperature, and P_{sig} is the output power of the oscillator having a tank-circuit element with quality factor Q, which is the mechanical quality factor for the case of an RP-OMO.

Meanwhile, the Q_o of the structure governs the optical field gradient that in turn sets the loop gain of the system, so must be at least high enough to initiate self-sustained oscillation. Here, the silicon nitride component of the Q-boosted RP-OMO provides a high-Q_o optical cavity that supports a whispering gallery mode resonance in which the optical field propagates along the silicon nitride ring's circumference. For maximum optical Q_o, the optical mode must not overlap with potential sources of optical loss, which dictates

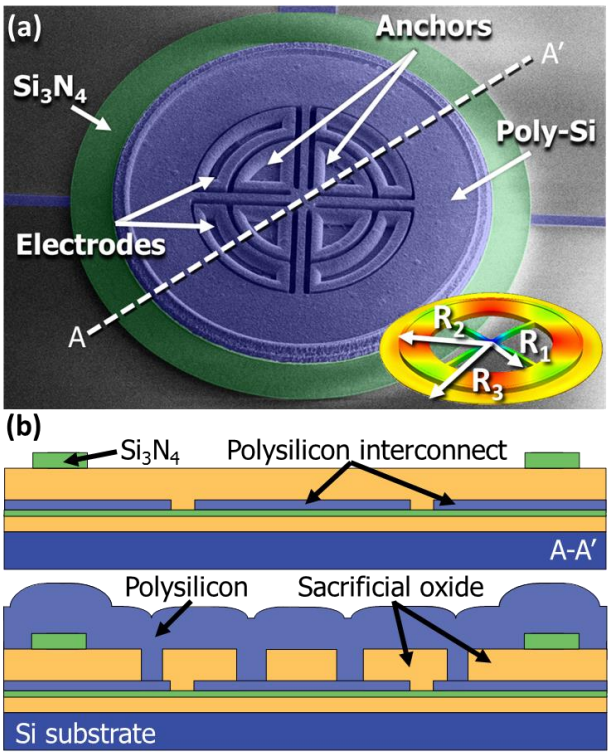

Fig. 4: (a) Colorized SEM image of the Q-boosted RP-OMO with an inset of mode shape by FEM simulation. R_1 and R_3 are the inner radius of polysilicon and outer radius of Si_3N_4 rings, respectively. R_2 represents the outer radius for polysilicon and inner radius for Si_3N_4 rings where both are coupled. (b) Summary of the fabrication process flow in which LTO and Si_3N_4 layers are deposited for electrical isolation and etch stop followed by polysilicon interconnect deposition and etch. Another LTO layer is deposited and CMP'ed to a final thickness of 2 µm, leaving a planar surface for the 500 nm Si_3N_4 film. After an anchor etch step, 2 µm of polysilicon is deposited and etched stopping on LTO or Si_3N_4. Finally, devices are released in 49% HF, yielding the final cross-section of Fig. 1(b).

a minimum distance between the scatter-prone polysilicon-nitride attachment interface and the outer edge of the nitride ring. On the other hand, for maximum mechanical Q_m (as will be seen), the width of the nitride ring should be minimized relative to that of the polysilicon one. The nitride ring width thus serves as a design parameter through which RP-OMO performance can be optimized.

MECHANICAL *Q*-BOOSTING

Again, the key to the phase noise performance obtained here is the high mechanical Q_m; and the key to the high Q_m is a concept introduced in [8] dubbed *Q*-boosting. *Q*-boosting is a mechanical circuit-based approach where a high-*Q* resonator raises the functional *Q* of a low-*Q* resonator in a mechanically coupled system by sharing its energy while adding relatively no loss [8]. In the multi-material RP-OMO, a higher Q_m polysilicon ring effectively supplies the added energy to a low Q_m (but high Q_o) nitride ring, where both vibrate together in the breathing contour mode shape depicted in the inset of Fig. 4(a).

Neglecting the loss at the nitride-polysilicon interface and possible change in the structure's anchor loss due to coupling of two materials, the functional mechanical $Q_{m,tot}$ of the composite structure can be expressed as:

$$Q_{m,tot} = \omega_m \frac{KE_{SiN} + KE_{pSi}}{E_{lost/cycle}} \tag{4}$$

where $E_{lost/cycle}$ is the total mechanical loss per cycle in the polysilicon and silicon nitride rings; and KE_{SiN} and KE_{pSi} are their respecitve kinetic energies, given by:

$$\begin{aligned} KE_{SiN} &= \frac{1}{2} \cdot m_{SiN} \cdot V_{R_2}^2 \\ KE_{pSi} &= \frac{1}{2} \cdot m_{pSi} \cdot V_{R_2}^2 \end{aligned} \tag{5}$$

where V_{R_2} denotes the radial velocity at radius R_2, m_{SiN} and m_{pSi} are effective lumped masses of the silicon nitride and polysilicon rings at the coupling location, respectively, given by $m_{eff} = 2U/\left(\omega_m^2 \cdot \Re^2(R_2)\right)$ with U being total stored energy in the mechanical mode, and $\Re(r)$ being radial displacement amplitude at radius r. Using (5) in (4) the functional $Q_{m,tot}$ simplifies to:

$$Q_{m,tot} = Q_{m,pSi} \frac{1 + \frac{m_{SiN}}{m_{pSi}}}{1 + \frac{m_{SiN}}{m_{pSi}} \cdot \frac{Q_{m,pSi}}{Q_{m,SiN}}} \tag{6}$$

which shows that the total $Q_{m,tot}$ of the RP-OMO structure depends on the Q_m and effective mass of both structures.

EXPERIMENTAL RESULTS

Fig. 4(a) presents a colorized SEM image of a fabricated *Q*-boosted RP-OMO together with the fabrication process. The doped polysilicon mechanical structure and inner capacitive gap electrodes are anchored and electrically connected to a thin layer of conductive polysilicon patterned on the substrate to serve as interconnects that facilitate electrical interrogation and read-out. The electrodes additionally allow tuning of the RP-OMO's oscillation frequency (such as needed for CSAC application [1]) via well-known voltage-controllable electrical stiffness [9].

Fig. 5(a) shows the experimental setup used to characterize the RP-OMO that basically employs the custom-built vacuum probe system of [1]. Measurement of Brownian noise shown in Fig. 5(b) reveals a multi-material RP-OMO boosted Q_m of 22,300, which is more than 2× higher than demonstrated in a previous silicon nitride RP-OMO [1]. To gauge the degree to which (6) matches the measured $Q_{m,tot}$ requires knowledge of the $Q_{m,pSi}$ of a spoke-supported polysilicon ring and the $Q_{m,SiN}$ of an unsupported nitride ring. The former is readily measured to be on the order of 48,000 on actual polysilicon spoke-supported rings operating in their first radial-contour modes [10]. The Q_m of an unsupported nitride ring, on the other hand, is much more elusive, since any real fabricated nitride ring does have supports, so

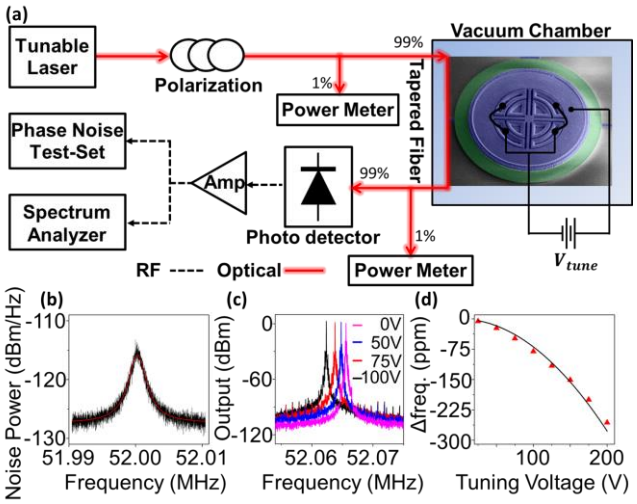

Fig. 5: (a) Schematic description of the experimental measurement setup. The RP-OMO is characterized in a custom-built vacuum chamber as described in [1]. An Agilent E5505A phase noise test system is used for phase noise measurements. (b) Measured Brownian motion of the RP-OMO from which Q_m=22,300 is extracted (c)-(d) demonstrate frequency tuning vs. applied tuning voltage and also (via curve-fitting) indicate a 440 nm resonator-to-electrode gap spacing.

suffers from anchor loss not present in an unsupported (levitated) ring. One reasonable approximation, however, might be the highest Q_m of 10,400 measured among several fabricated spoke supported 1st radial-contour mode nitride rings [1] at the frequency of interest. With the above Q_m values and 2.51 ng nitride and 5.91 ng polysilicon effective masses calculated from the device dimensions given in Fig. 6, Eq. (6) predicts a $Q_{m,tot}$ of 23,100 for the composite RP-OMO which agrees well with the measured value of 22,300.

Fig. 5(c) and (d) present RP-OMO output spectra under several tuning voltages and measured plots gauging oscillating RP-OMO frequency versus tuning voltage, where a relatively large 440 nm electrode-to-resonator gap spacing still allows a 3 ppm/V frequency shift suitable for locking to the Rb vapor cell in a CSAC.

Fig. 6 presents the measured phase noise for the *Q*-boosted RP-OMO of -125 dBc/Hz at 5 kHz offset from its 52-MHz carrier, which is 12 dB better than the previous state of the art RP-OMO constructed of silicon nitride alone [1], despite the use of an input laser power of only 3.6 mW—more than 2× smaller than that of the previous state-of-the-art [1].

CONCLUSIONS

A multi-material RP-OMO structure has been shown to boost the Q_m of a silicon nitride RP-OMO by more than 2× toward realization of the simultaneous high Q_m >22,000 and Q_o >190,000 needed to maximize RP-OMO performance. The *Q*-boosted RP-OMO bests the previous state-of-the-art by reducing the phase noise at 5 kHz offset from the carrier by a measured 12 dB that matches the prediction of Eq. (3) with the improved Q_m. The design is shown to have little or

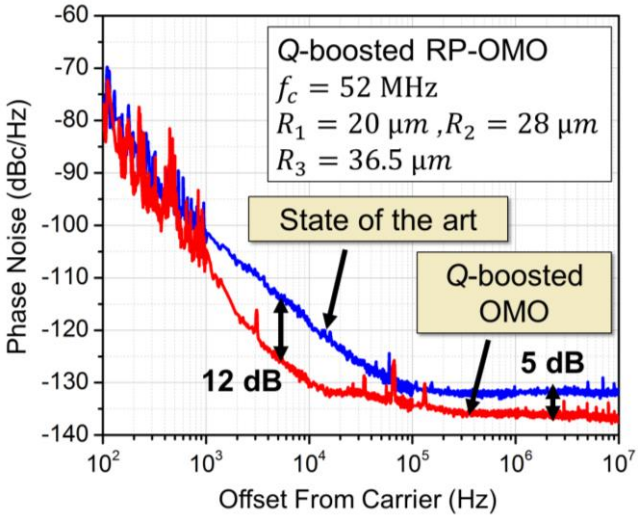

Fig. 6: Phase noise spectra of the Q-boosted RP-OMO compared to the previous best Si_3N_4-only RP-OMO [1]. As expected, the enhanced Q_m lowers the phase noise, achieving a 12 dB improvement at 5 kHz offset.

no effect on the optical properties of the high Q_o silicon nitride, allowing retention of high Q_o despite the introduction of a scatter-prone material interface in the vicinity of the optical resonance. While polysilicon is chosen for its high Q_m in the RP-OMO of this work, the design is applicable to any material of choice as long as it can be integrated with another high Q_o material of choice. The use of high Q_m doped polysilicon as one of the materials further enables electrical interrogation and readout of the RP-OMO, as well as an electrical stiffness-based voltage controlled frequency tuning very much needed for locking in a target low-power CSAC application [1].

Acknowledgement: This work was supported under the DARPA ORCHID program.

REFERENCES

[1] T. O. Rocheleau et al., *Proceedings, IEEE Int. Conf. on MEMS*, 2013, pp. 118-121.
[2] A. Schliesser et al., *Phys. Rev. Lett.*, vol. 97, no. 24, pp. 243905(4), 2006.
[3] H. Rokhsari et al., *Opt. Express*, vol. 13, no. 14, pp. 5293-5301, 2005.
[4] T. J. Kippenberg et al., *Science*, vol. 321, pp. 1172-1176, 2008.
[5] M. Hossein-Zadeh et al., *IEEE J. Sel. Topics Quantum Electron.*, vol. 16, no. 1, pp. 276-287, 2010.
[6] J. C. Knight et al., *Opt. Lett.*, vol. 22, no. 15, pp. 1129-1131, 1997.
[7] D. B. Leeson, *Proc. IEEE*, vol. 54, pp. 329-330, 1966.
[8] Y. W. Lin et al., *in Dig. of Tech. Papers Transducers'07*, pp. 2453-2456.
[9] H. Nathanson et al., *IEEE Trans. Electron Devices*, vol. 14, no. 3, pp. 117-133, 1967.
[10] S.-S. Li et al., *Proceedings, IEEE Int. Conf. on MEMS*, 2004, pp. 821-824.